Invasion Percolation on Correlated and Elongated Lattices

Knackstedt, Mark A.; Marrink, S.J.; Sheppard, Adrian P.; Pinczewski, W.V.; Sahimi, Muhammad

Published in:
Transport in Porous Media

DOI:
10.1023/A:1010770010309

Transport in Porous Media **44:** 465–485, 2001.

Invasion Percolation on Correlated and Elongated Lattices: Implications for the Interpretation of Residual Saturations in Rock Cores

MARK A. KNACKSTEDT[1,2,⋆], S. J. MARRINK[1,2], ADRIAN P. SHEPPARD[1,2], W. V. PINCZEWSKI[2] and MUHAMMAD SAHIMI[3]
[1]*Department of Applied Mathematics, Research School of Physical Sciences and Engineering, Australian National University, Canberra ACT 0200, Australia*
[2]*School of Petroleum Engineering, University of New South Wales, Sydney, NSW 2052, Australia*
[3]*Department of Chemical Engineering, University of Southern California, Los Angeles, CA 90089-1211*

(Received: 16 November 1999)

Abstract. The invasion percolation model is used to investigate the effect of correlated heterogeneity on capillary dominated displacements in porous media. The breakthrough and residual saturations are shown to be strongly influenced by the correlations. Correlated heterogeneity leads to lower residual saturations than those observed in random systems and the scatter commonly observed in laboratory core measurements of the residual saturations can be attributed to the presence of such heterogeneity at the pore scale. Invasion percolation computations on elongated lattices, those with a geometry of $L^{d-1} \times nL$ where n denotes the aspect ratio, show that residual saturations for systems with correlated heterogeneity exhibit a strong dependence on aspect ratio. This effect is not considered by experimentalists who advocate the use of long (high aspect ratio) cores in order to overcome 'end-effects' in experiments on shorter cores. A new scaling law is proposed for the residual saturations in elongated systems with correlated heterogeneity, and is confirmed by numerical simulations.

Key words: Two-phase flow, correlated heterogeneity, invasion percolation.

1. Introduction

The study of multiphase flow phenomena in sedimentary rocks is relevant to many problems of industrial importance including transport of non-aqueous contaminants in groundwater and the production of oil and gas from sedimentary reservoirs. In oil and gas recovery from petroleum reservoirs, an area of particular interest to the authors, recovery depends on residual saturation – the volume fraction of the pore space occupied by oil or gas which cannot be recovered because it is trapped or bypassed in the reservoir rock by the combined effects of capillary forces and heterogeneity. Realistic estimation of residual saturations is a central problem in the development of new fields and in improving recoveries from existing fields.

⋆ Corresponding author: mak11ø@rsphysse.anu.edu.au

Residual saturations cannot be predicted *a priori* and current industry practice is to make measurements on small core plugs (at length scales of order of cm) and use these to calibrate *in situ* wireline log measurements (at length scales of order of meters). Implicit in this scale-up procedure is the assumption that rock structure is random.

Percolation theory (Sahimi, 1993; Stauffer and Aharony, 1994) has been used (Larson and Scriven, 1977; Sahimi, 1993) to explain residual or trapped fluid saturations in two-phase displacements, where the amount of residual fluid is analogous to the percolation threshold p_c. In most previous applications of percolation theory, spatial disorder has been assumed to be uncorrelated. However, it has recently been suggested that long-range correlations are likely to exist in many porous sedimentary rocks (Hewett, 1986; Painter and Paterson, 1994; Painter, 1995, 1996; Sahimi *et al.*, 1995; Makse *et al.*, 1996; Mehrabi *et al.*, 1997; Knackstedt *et al.*, 1998; Sahimi, 1998). This has encouraged studies of percolation on correlated lattices (Schmittbuhl *et al.*, 1993; Du, 1996; Sahmi and Mukhopadhyay, 1996; Marrink *et al.*, 1999). Results of such simulations on correlated systems show that correlation has a significant effect on the percolation threshold and the threshold is no longer unique but depends on the spanning rule employed (Marrink *et al.*, 1999). Previous studies of invasion percolation (IP), the model most applicable to the study of capillary-dominated displacment in porous media, on correlated lattices have been limited to two dimensions (Meakin, 1991; Wagner *et al.*, 1997) and have only considered saturations up to breakthrough point, that is, the point at which the displacing fluid spans the system for the first time, and also the fractal properties of the fluid clusters (Knackstedt *et al.*, 2000). These studies provide no information on the manner in which residual saturation may scale in actual porous media which display correlated heterogeneity.

In this work we use the IP model to investigate the effect of correlated heterogeneity on capillary dominated displacements in porous media. The breakthrough and residual saturations are shown to be strongly dependent on the degree of correlation. The results show that correlated heterogeneity leads to substantially lower residuals than observed on random lattices. The large scatter in the residual saturation commonly observed in laboratory core measurements can be attributed to the presence of correlated heterogeneity at the pore scale. Laboratory measurements on reservoir rocks are commonly made on core samples of high aspect ratios. We therefore investigate the effect of aspect ratio on the residual saturations. We find that theoretical predictions derived previously (Marrink and Knacktstedt, 1999; 2000) for the finite-size scaling of the saturations for random percolation (RP) on elongated lattices can be extended to IP. We then extend this scaling analysis to systems exhibiting correlated heterogeneity. Implications of correlated heterogeneity on the interpretation of laboratory displacement experiments on rock cores are discussed.

The plan of the paper is as follows. In the next section we describe the simulation methods and the generation of lattices with correlated heterogeneity. In

Section 3 we present results of IP simulations on cubic lattices with varying degrees of correlated heterogeneity. In Section 4 we review our previous work on the finite-size scaling of the percolation threshold for RP and extend the scaling theory for elongated random lattices to correlated lattices. We also present results of IP simulations with correlated heterogeneity on elongated lattices. Section 5 summarizes the implications of the results for the interpretation of laboratory immiscible displacement experiments.

2. Numerical Implementation

2.1. INVASION PERCOLATION SIMULATION

We consider the IP model in three dimensions on a simple-cubic lattice. The standard IP simulations begin by assigning a number to each site of the lattice from an arbitrary random distribution, where each site's number is not correlated with those of its neighbors. Initially the lattice is filled with the defending fluid and the invading fluid occupies one edge or face of the lattice. At each step in the simulation the site with the largest value on the interface between the invading and defending phases is occupied by the defender. Two main variants of IP have been studied. In the first, compressible IP (CIP), the defending fluid is compressible and the invading fluid can potentially invade any region on the interface occupied by defending fluid. In the second and more realistic model in the context of displacements in porous media, trapping IP (TIP), the defending fluid is incompressible and can be trapped when a portion of it is surrounded by the invading fluid.

For TIP simulations, the defending fluid is considered trapped when it becomes disconnected from the exit face. The breakthrough saturation S_I is defined as the volume fraction of the invading fluid when it spans the system for the first time, and the residual saturation S_r is defined as the saturation of the defending fluid when it can no longer flow from the exit face. To mimic laboratory measurements we use reflecting boundary conditions and report results measured along the full lattice. In all cases we consider thresholds along a specified direction. In particular, for elongated lattices we consider the thresholds along the direction of extension.

We utilise a new algorithm which allows rapid simulation of IP (Sheppard and Sok, submitted). In the conventional algorithms the search for the trapped regions is done after every invasion event using a Hoshen–Kopelman algorithm (Hoshen and Kopelman, 1976), which traverses the entire lattice, labels all the connected regions, and then only those sites that are connected to the outlet face are considered as potential invasion sites. A second sweep of the lattice is then done to determine which of the potential sites is to be invaded in the next time step. Thus, each invasion event demands $O(N^2)$ calculations, where N is the number of sites in the lattice. This is highly inefficient for two reasons. First, after each invasion event only a small local change is made to the interface; implementing the global Hoshen–Kopelman search is unnecessary. Secondly, it is wasteful to traverse

the entire network at each time step to find the most favorable site (bond) on the interface since the interface is largely static.

We tackle the first problem by searching the neighbours of each newly invaded site (bond) to check for trapping. This is ruled out in almost all instances. If trapping is possible, then several simultaneous breadth first 'forest-fire' searches are used to update the cluster labelling as necessary. This restricts the changes to the most local region possible. Since each site (bond) can be invaded or trapped at most once during an invasion, this part of the algorithm scales as $O(N)$. The cluster searching method used here has some similarities with the 'perimeter scouting' algorithm (Meakin, 1991) for 2D clusters. In this algorithm one checks whether the most recently invaded sites could have been trapped in the interior of the cluster. If so, oriented walks are started on the just invaded site, pointing away from it to the neighboring sites which are those that neither belong to the cluster nor are candidates for invasion. The walks continue until all but one of them have again reached the site of origin. The growth sites visited by these walks are then eliminated from the list of active sites. This method is effective in 2D but not as efficient in 3D. Our method differs from it by searching cluster volumes rather than perimeters, and incorporating local checking to minimize cluster searching and is thus equally effective in 3D.

The second problem is solved by storing the sites on the fluid–fluid interface in a list, sorted according to the capillary pressure threshold (or size) needed to invade them. This list is implemented using a balanced binary search tree, so that insertion and deletion operations on the list can be performed in $\log(n)$ time, where n is the list size. The sites that are designated as trapped using the procedures described above are removed from the invasion list. Each site (bond) is added and removed from the interface list at most once, limiting the computational effort of this part of the algorithm to $O[N \log(n)]$. Thus, the execution time for N sites is dominated (for large N) by list manipulation and scales at most as $O[N \log(N)]$.

While the execution time is approximately $O[N \log(n)]$, in practice the time and memory requirements depend on the total number of lattice sites and those forming the cluster boundary. For example, we find empirically that for 3D TIP the execution time scales as $N^{1.24}$, and the memory use is 20 bytes for each lattice site plus 64 bytes for each cluster site. On a 500 MHz 21164A Alpha microprocessor, a trapped cluster of 2×10^5 sites is grown on a $181 \times 181 \times 181$ lattice in 12.0 s, using 120 Mb of memory, while in 2D a cluster of 5×10^5 sites is grown on a 2000×2000 lattice in 12.0 s, using only 52 Mb. Complete details of the algorithm, which can be used for arbitrary networks, are given elsewhere (Sheppard and Sok, submitted; Sheppard *et al.*, 1999).

2.2. GENERATION OF CORRELATED LATTICES

Heterogeneity in geological formations is likely to exist at all length scales. Hewett (Hewett, 1986) has shown that at large (field) scales heterogeneity is correlated and

may be approximated by a fractional Brownian motion (fBm). Following Hewett, we generate correlated fields based on fBm. A feature of a network of pores with a statistical descripted based on a fBm is that it contains long-ranged correlations in pore sizes, with the variance of the pore size give by, $\langle r(\mathbf{x}) - r(\mathbf{x_0})\rangle = C_0|\mathbf{x} - \mathbf{x_0}|^{2H}$, where C_0 is a constant and the type and extent of the correlations can be tuned by varying H. This contrasts with random lattices where adjacent pore sizes are independent. Recent work (Knackstedt *et al.*, 1998) comparing experiments on Berea sandstone and simulation of porosimetry (an IP process) on correlated lattices suggests that correlated heterogeneity exists down to the pore scale and that at this scale correlations persist at scales up to several pore lengths. We therefore introduce a cutoff length scale ℓ_c such that, $\langle r(\mathbf{x}) - r(\mathbf{x_0})\rangle = C_0|\mathbf{x} - \mathbf{x_0}|^{2H}$ for $|\mathbf{x} - \mathbf{x_0}|\langle\ell_c$, and $\langle r(\mathbf{x}) - r(\mathbf{x_0})\rangle = C_0|\ell_c|^{2H}$ for $|\mathbf{x} - \mathbf{x_0}|\rangle\ell_c$. The introduction of ℓ_c allows us to choose an appropriate length scale for correlations at the pore scale.

3. Numerical Results on Cubic Lattices

3.1. SATURATIONS

In this section we describe the effect of correlated heterogeneity on estimates of breakthrough and residual saturations and on the variance of these estimates on a cubic lattice. We first illustrate the effect of lattices with correlated heterogeneity on the structure of TIP clusters at the breakthrough. Figure 1 shows examples of configurations in two dimensions at the breakthrough threshold for an uncorrelated lattice and for correlated lattices at three specific values of the Hurst exponent H. For the correlated lattices we show two cases; one for a cutoff length in the correlations of $\ell_c = 8$ and a second case for which $\ell_c = L$ so that the extent of the correlations is as large as the linear size of the system. Clearly, with increasing H the compactness of the cluster changes and the distribution of the trapped phases is altered. The same qualitative changes are evident in 3D displacements.

The breakthrough of the injected phase in invasion percolation is described by

$$S_I = AL^{-(D-d_f)} \tag{1}$$

where D is the Euclidean dimension and d_f is the fractal dimension of the invading cluster. Values of d_f for systems with correlated and uncorrelated properties are given in Table I (Knackstedt *et al.*, 2000). The estimate for uncorrelated networks is more accurate than any previously published result and agrees with previous estimates (Sahimi, 1994; Wilkinson and Willimsen, 1983). Results on correlated lattices (Knackstedt *et al.*, 2000) show that for all $H < 0.5$ the fractal dimension of the invading cluster is dependent on H and there is an increase in d_f with increasing H. For all $H > 0.5$ the cluster at the breakthrough is compact ($d_f = D$). For the case of systems where we introduce a cutoff length scale ℓ_c, we observe (Knackstedt *et al.*, 2000) a crossover from the fractal behaviour associated with uncorrelated networks for length scales $\ell \gg \ell_c$ to the H-dependent $d_f(H)$ for $\ell < \ell_c$.

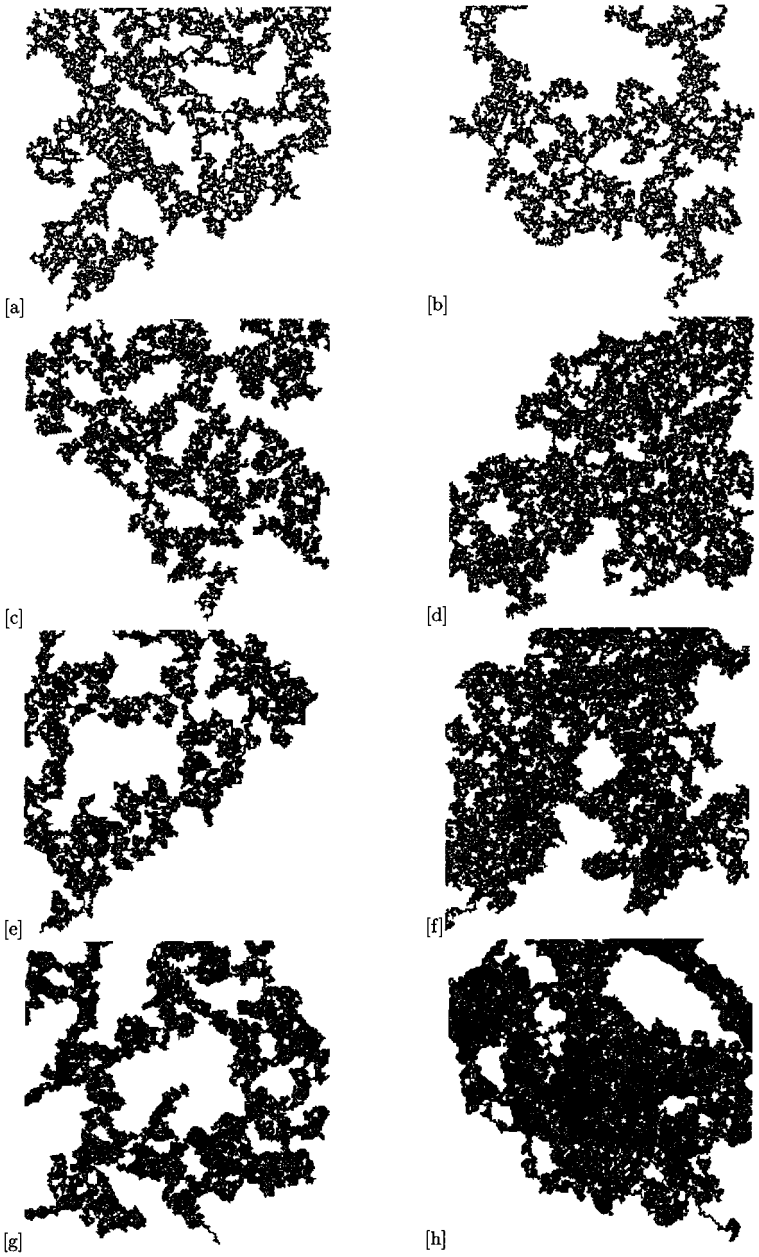

Figure 1. Examples of two dimensional TIP clusters at breakthrough illustrating the effect of correlated heterogeneity on cluster structure, (a), (b) random; (c) H=0.2, $\ell_c = 8$; (d) H=0.2, $\ell_c = \infty$; (e) H=0.5 $\ell_c = 8$; (f) H=0.5 $\ell_c = \infty$; (g) H=0.8, $\ell_c = 8$; (h) H=0.8, $\ell_c = \infty$.

Table I. Cluster fractal dimensions as a function of H (from Knackstedt *et al.*, 2000)

Correlation	$d_f(D=3)$
uncorrelated	2.524 ± 0.003
(previous estimates)	2.52 ± 0.01 [25]
$H = 0.1$	2.72 ± 0.01
$H = 0.2$	2.76 ± 0.01
$H = 0.3$	2.82 ± 0.02
$H = 0.4$	2.89 ± 0.01
$H = 0.5$	2.95 ± 0.02
$H = 0.6$	2.99 ± 0.02
$H = 0.9$	3.00 ± 0.01

Values of the residual saturation obtained for uncorrelated and correlated lattices are given in Figure 2 for different H and ℓ_c over a range of L. The spread in the data is due to variation in the pore size distribution for correlated lattices and is not due to insufficient numerical sampling. Finite-size scaling of the residual saturation for uncorrelated lattices was fitted to the following relationship:

$$S_r(L) = S_r(\infty) + cL^{-a}. \tag{2}$$

For the uncorrelated system we find $a = 1/\nu \simeq 1.14 \pm 0.02$, in good agreement with the exponent for RP without trapping ($\nu \simeq 0.88$). The finite-size scaling relationship allows one to predict the residual saturation of an infinite system; we obtain a value of $S_r(L \to \infty) \simeq 0.3402 \pm 0.0003$. The finite-size scaling behaviour for the correlated lattices is also evaluated at scales up to $L = 128$ and an example is shown in Figure 3 for $H = 0.8$. The asymptotic predictions of $S_r(L \to \infty)$ are given in Table II along with the value of the scaling exponent a. It should be noted that the exponent associated with the finite size scaling is significantly different from $1/\nu$ observed for RP.

From the results for the residual saturations we make the following observations. First, the introduction of correlations leads to a large reduction in the observed residual saturation. The value of the residual phase saturation is smaller for large H and generally decreases with increasing ℓ_c. However, the residual can show a minimal value for finite ℓ_c. This small increase of the residual at larger cutoff scales may be due to the possibility of trapping very large regions of the defending fluid at larger ℓ_c. Remarkably, the reduction in S_r is significant for correlations even at a small scale. For example, for a system with only a nearest-neighbor correlation $\ell_c = 2$ and $H = 0.8$ the residual saturation drops from 0.34 to 0.26, a decrease of over 20%. Small-scale correlations clearly have a profound effect on resultant saturations even at large scales.

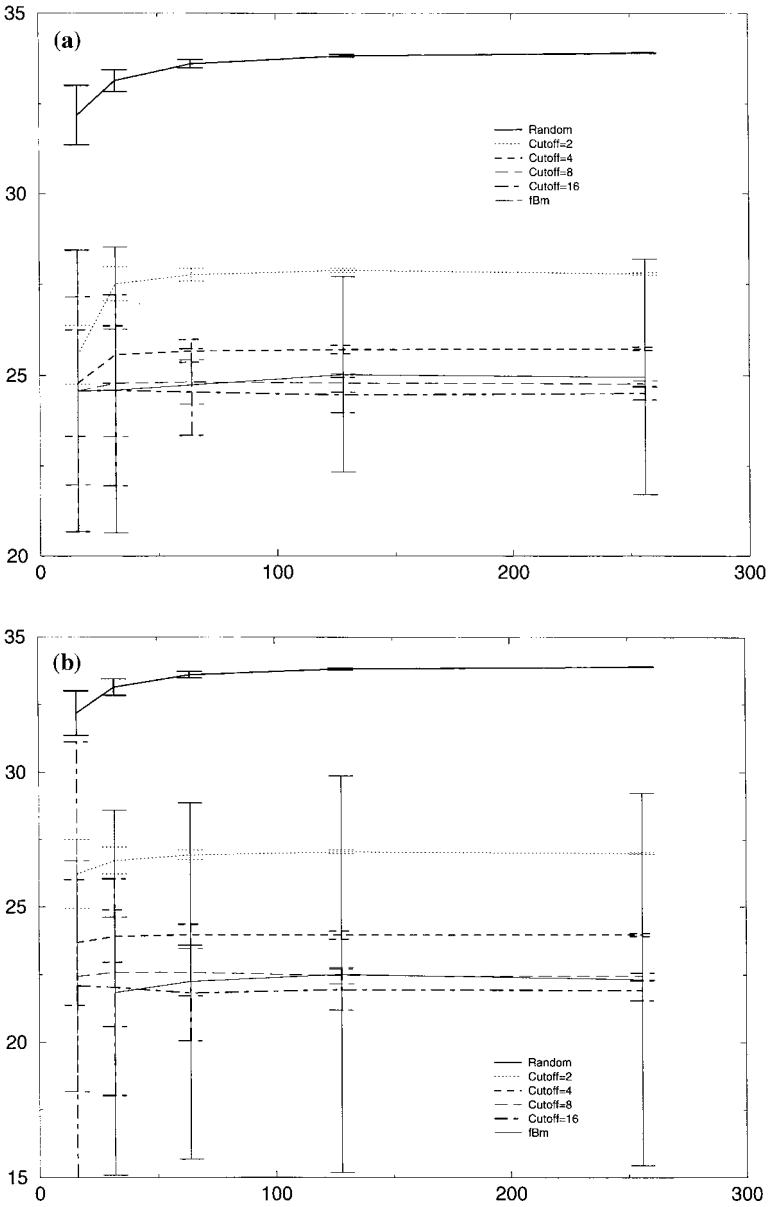

Figure 2. Residual saturations for correlated lattices for a range of ℓ_c. (a) $H = 0.2$; (b) $H = 0.5$; (c) $H = 0.8$.

3.2. CLUSTER SIZE DISTRIBUTION

The cluster size distribution of the trapped phase is also of great interest in the study of immiscible displacement processes. We have studied the size distribution of trapped clusters at the residual saturation point. We find that the distribution is strongly affected by the type and extent of correlation. In Figure 4 we show the

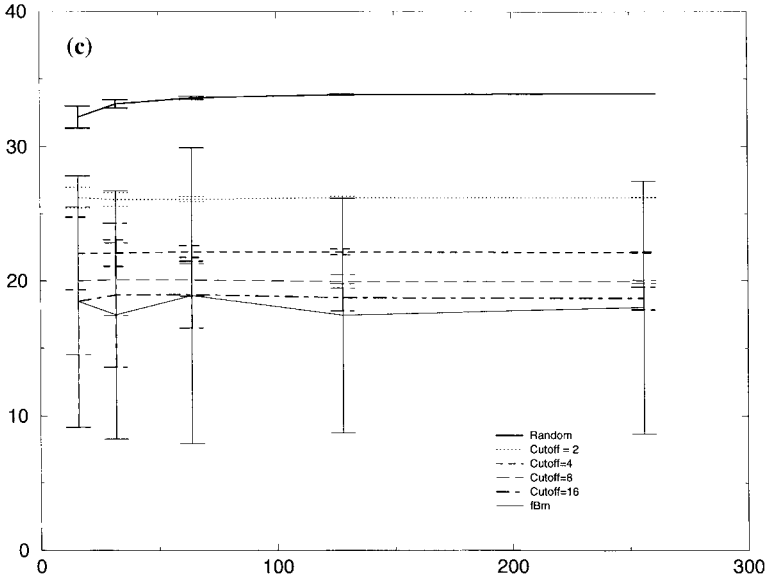

Figure 2. (*continued*)

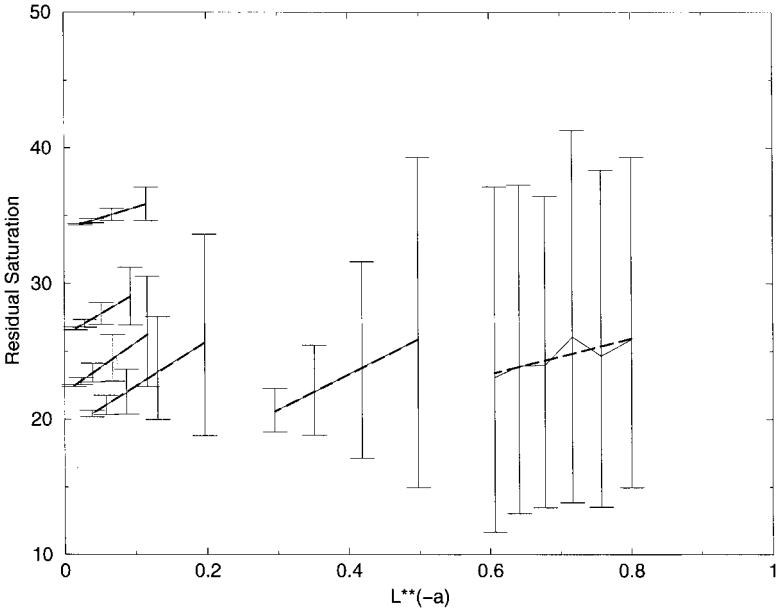

Figure 3. Finite size scaling of the residual saturation for an correlated grids with $H = 0.8$. The upper curve is for an uncorrelated lattice. Curves for $\ell_c = 2$, $\ell_c = 4$, $\ell_c = 8$, $\ell_c = 16$, and $\ell_c = \infty$ follow from upper left to bottom right. The fits to the values are good for all H. Values of the asymptotic saturations and the scaling exponent a are given in Table II.

Table II. Residual phase saturations and variability for different correlated lattices with various ℓ_c. numerical predictions are given along with the value of exponent a in Equation (2). For comparison, the value of S_r for a random lattice is 0.3400 with $a = 1.14$

	$H = 0.2$		$H = 0.5$		$H = 0.8$	
	$S_r(\infty)$	a	$S_r(\infty)$	a	$S_r(\infty)$	a
$\ell_c = 2$	0.278 ± 0.0003	0.85	0.271 ± 0.0003	0.93	0.262 ± 0.0003	0.86
$\ell_c = 4$	0.257 ± 0.0005	0.62	0.240 ± 0.0006	0.65	0.219 ± 0.0007	0.78
$\ell_c = 8$	0.248 ± 0.0008	0.50	0.225 ± 0.0012	0.55	0.128 ± 0.001	0.58
$\ell_c = 16$	0.245 ± 0.002	0.32	0.222 ± 0.0035	0.36	0.158 ± 0.008	0.25
fBm	0.250 ± 0.03	0.22	0.223 ± 0.065	0.18	0.180 ± 0.094	0.08

number of residual clusters of size s for a correlated system with $H = 0.5$ and different values of the cutoff length ℓ_c. We plot $n_s(s)$, the number of clusters of size s. For RP one expects (Stauffer and Aharony, 1994; Sahimi, 1994) $n_s(s)$ to follow the following scaling law:

$$n_s(s) \propto s^{-\tau}, \tag{3}$$

where $\tau \simeq 2.18$. A more accurate way of measuring the cluster size statistics is [27] by investigating $N_s(s) = \sum_{s'>s} s' n_{s'}$, the average total number of clusters with a size greater than a given size s. In general one expects to have

$$N_s(s) \propto s^{2-\tau}. \tag{4}$$

If there are no long-range correlations in the system, percolation theory predicts that the exponent τ is universal. Since the 3D spanning cluster for TIP with no long-range correlations has the same fractal dimension as that of RP, we expect the uncorrelated case and the cases with a finite ℓ_c to show this scaling behaviour; this is observed in Figure 4. For the system with long-range correlations ($\ell_c \geqslant L$) d_f is nonuniversal and depends on H (Knackstedt *et al.*, 2000). We therefore observe nonuniversal values of τ that depend on H for $\ell_c \geqslant L$.

We can, however, make some observations on the size of the trapped clusters as a function of ℓ_c. For small ℓ_c there is only a small effect on the distribution of the trapped phase. For intermediate and larger values of ℓ_c we observe a higher proportion of the trapped sites lie in larger trapped clusters. For the case $\ell_c \to \infty$ one single trapped cluster dominates over 30% of the residual phase.

The dynamics of the trapping is also strongly dependent on the presence of correlated heterogeneity. We plot in Figure 5 the total proportion of trapped clusters as a function of saturation. We see very different dynamics when comparing random and correlated systems. In the random system, trapping occurs only near the end of the invasion – when over 80% of the total invading fluid is present and less than 5% of the defender is trapped. In contrast, when we introduce a cutoff of, for example, $\ell_c = 16$, over 30% of the defending fluid is trapped at 80% invader saturation.

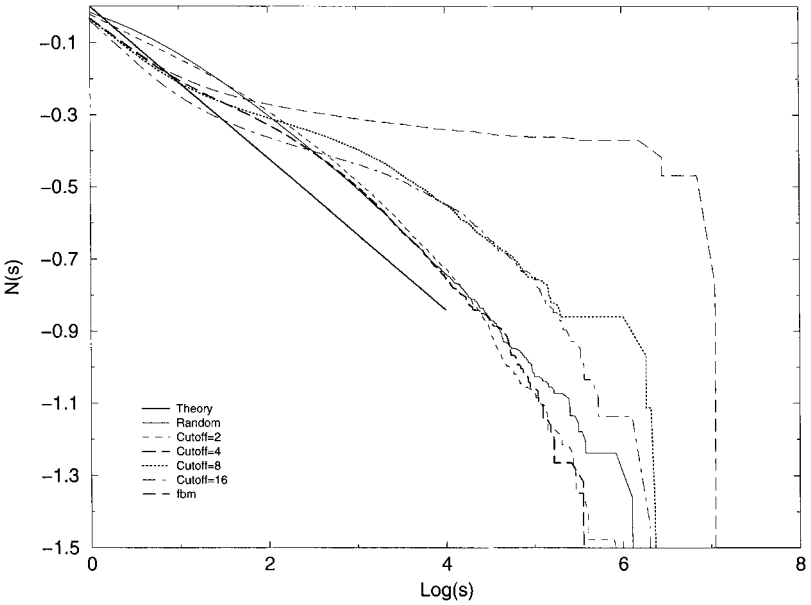

Figure 4. Size distribution of the trapped clusters as a function for $H = 0.5$ as a function of ℓ_c. Plotted on the y-axis is the log of the cumulative cluster size distribution $log(N_s(s))$ versus $log(s)$, where $N_s(s) = \sum_{s>} sn_s$, the average total number of clusters with a size greater than a given size s. In the uncorrelated case and for finite ℓ_c we see that the scaling predicted from RP holds. For the case of infinite correlations, the scaling behaviour differs strongly. Note that for the fBm field one trapped cluster has a huge proportion of the trapped phase and more than half the trapped phase lies within a few trapped clusters. However, the proportion of small trapped clusters is also large.

3.3. VARIABILITY IN MEASUREMENT

Each realisation of the IP process gives a numerically different result. It has been a common practice on simulated data to examine the average results over thousands of realisations. However, laboratory core measurements are necessarily performed on only a small number of samples, so it is of interest to consider the variability between realisations. Variability is of physical significance because it provides an indication of the scatter which should be expected to occur in laboratory measurements.

For the uncorrelated lattice, percolation theory predicts that the variation in the threshold will scale according to

$$\sigma(L) \propto L^{-b}, \tag{5}$$

where $b = 1/\nu$ for RP, and ν is the critical exponent of the percolation correlation length. We find Equation (5) to hold for TIP on an uncorrelated lattice. In Table III we report the scaling exponent b of Equation (5) for the correlated lattices with finite ℓ_c. Most values are close to but slightly larger than the RP prediction of

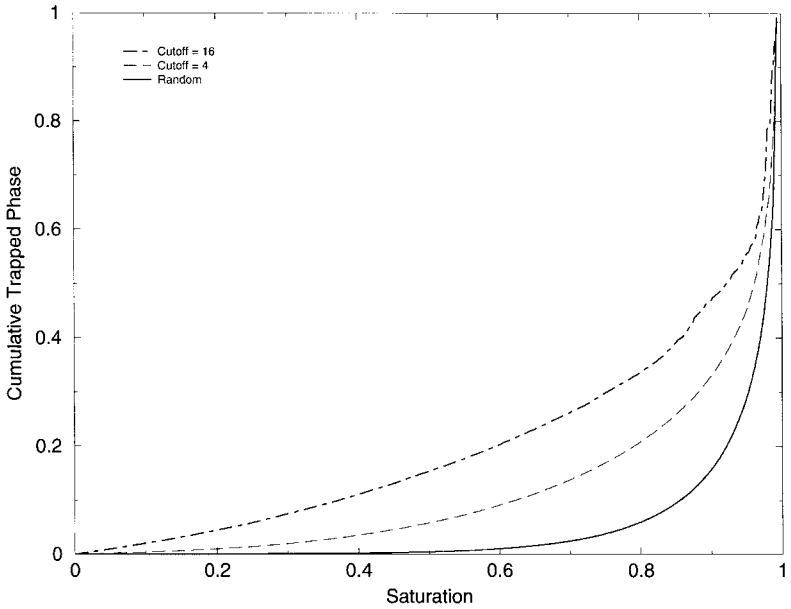

Figure 5. Proportion of trapped phase as a function of total invading phase saturation. In the random system all trapping occurs at the end of the invasion. In contrast for finite ℓ_c much of the defending phase is trapped at earlier stages of the invasion.

Table III. Scaling exponent a of the standard deviation of the residual saturation with L

	$H = 0.2$	$H = 0.5$	$H = 0.8$
$\ell_c = 2$	1.25	1.36	1.20
$\ell_c = 4$	1.26	1.34	1.36
$\ell_c = 8$	1.24	1.30	1.31
$\ell_c = 16$	1.12	1.30	1.07

$1/\nu \simeq 1.14$. In this case the data are close to the RP result and it is difficult to draw quantitative conclusions whether they differ significantly. However, the scaling exponent for the standard deviation differs significantly from the scaling exponent of the saturation.

As seen in Figure 2, the standard error of the residuals for fully correlated lattices ($\ell_c = \infty$) is independent of L. In Figure 6 we show individual realisations for the fully correlated lattices illustrating the wide variation in the observed residuals even at large L. The data also shows the large skew in the data to higher values of the saturations. Clearly, for correlated systems the distribution of thresholds deviates strongly from a Gaussian. Morevoer, the individual realisations show ex-

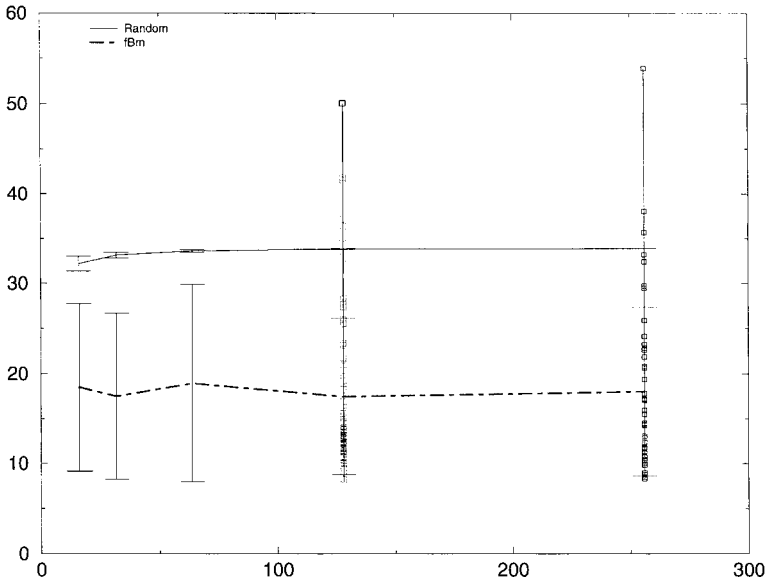

Figure 6. Individual variability in the measured residual phase saturation for a lattice with long-range correlations. A comparison to an uncorrelated lattice is shown. The fully correlated lattices exhibit a wide variation in the observed residuals even at large L. Clearly a small number of measures on a correlated grid will lead to poor estimation of residual saturation. The data is also skewed showing the poor fit to a Gaussian distribution (see Figure 9).

plicitly that measurements on a small number of samples on a correlated lattice will lead to poor estimation of residual saturation. This result highlights the need to experimentally measure on core sizes L that are larger than the length scale of the correlated heterogeneity ℓ_c. As discussed above, the variance of the residuals decreases quickly with exponent L as L^{-a} with $a > 1$. From this result and from visual inspection of Figure 2 we expect that variances in the measured residuals for $L/\ell_c > 10$ are small. This result implies that measurements of residuals should be made on sample sizes that are at least 10 times larger than the extent of correlation.

4. Saturations on Elongated Lattices

We now consider the properties of an elongated lattice, that is, those with dimensions of $L^2 \times nL$, where n denotes the aspect ratio of the lattice. Laboratory measurements on long cores (high aspect ratio) are commonly used to minimise entry and exit effects which may influence measurements on short (low aspect ratio) cores. The interpretation of such laboratory measurements requires an understanding of the effect of aspect ratio on the residual saturation.

4.1. SCALING THEORY FOR SATURATIONS ON ELONGATED LATTICES

4.1.1. *Scaling Theory for Random Elongated Lattices*

In recent work (Marrink and Knackstedt, 1999) we have derived scaling laws for residual saturation on elongated lattice for random percolation. We briefly review the results for the expectation value of the spanning cluster density and the percolation threshold for RP as they are related to the breakthrough and the trapping thresholds for IP.

For finite lattices the realised values of the percolation threshold are distributed around its expectation value $\langle p_c \rangle$ and for L large enough the probability distribution P of having a lattice percolating at p approximately approaches a Gaussian distribution*

$$P = \frac{1}{\sigma(L)\sqrt{2\pi}} e^{(-x^2)}, \tag{6}$$

with $x = (p_c(L) - \langle p_c(L) \rangle)/(\sqrt{2}\sigma(L))$ and $\sigma(L)$ denotes the standard deviation of the distribution. Now consider an elongated lattice consisting of n independent cubic lattices linked together. Each of the sublattices percolates at a percolation threshold $p_c(L)$ according to the probability distribution P. The percolation threshold $p_c^{\text{ext}}(n, L)$ of the elongated lattice (specified along the direction of extension) is now determined by the cubic lattice with the highest percolation threshold; this lattice forms the 'bottleneck' to percolation of the elongated lattice.

In previous work (Marrink and Knackstedt, 1999; 2000) we showed that the probability $P^{\text{ext}}[p_c{}^{\text{ext}}(n, L)]$ that an elongated lattice percolates below $p_c^{\text{ext}}(n, L)$ is given by the product of $2n - 1$ independent probabilities $P(p_c(L))$, that is,

$$P^{\text{ext}}[p_c^{\text{ext}}(n, L)] = \{P[p_c(L)]\}^{2n-1}, \tag{7}$$

and that the expectation value of the percolation threshold for RP on an elongated lattice of aspect ratio n, $p_c^{\text{ext}}(n, L)$, can be expressed approximately as

$$\langle p_c^{\text{ext}}(n, L) \rangle = \langle p_c(L) \rangle + \sqrt{2}\sigma(L)\sqrt{\ln n}. \tag{8}$$

The fit of Equation (7) and Equation (8) to numerical data for RP is excellent (Marrink and Knackstedt, 1999; 2000).

4.1.2. *Scaling Theory for correlated elongated lattices*

We now extend the scaling behaviour derived for the residual saturations for percolation on random lattices to correlated systems. When a system is generated with correlated heterogeneity, a Gaussian distribution no longer describes $P(p_c)$

* It has been shown that the distribution of percolation thresholds deviates slightly from Gaussian (Ziff, 1994; Haas, 1995).

accurately. Fits to the probability distribution P for large p are now given by the more general form

$$P(p, L) = 1 - F(x)\exp(-x^a), \tag{9}$$

where $F(x) = bcx^{1-a}/a$ denotes an algebraic correction to the leading decay, $x = (p - \langle p_c(L)\rangle)/b$, and $x_0 = -\langle p_c(L)\rangle/b$. The Gaussian distribution with standard deviation $\sigma(L)$ (see Equation (6)) corresponds to the case, $a = 2, b = \sqrt{2}\sigma(L)$, and $c = 1/(b\sqrt{\pi})$. For an elongated lattice of n sublattices linked together, each percolating according to P given in Equation (9), and the modified expectation value for $< p_c^{\text{ext}} >$ is to first order

$$< p_c^{ext} >=< p_c > +\sqrt{2}\sigma(\ln n)^{1/a}. \tag{10}$$

For a Gaussian ($a = 2$) distribution we recover Equation (8).

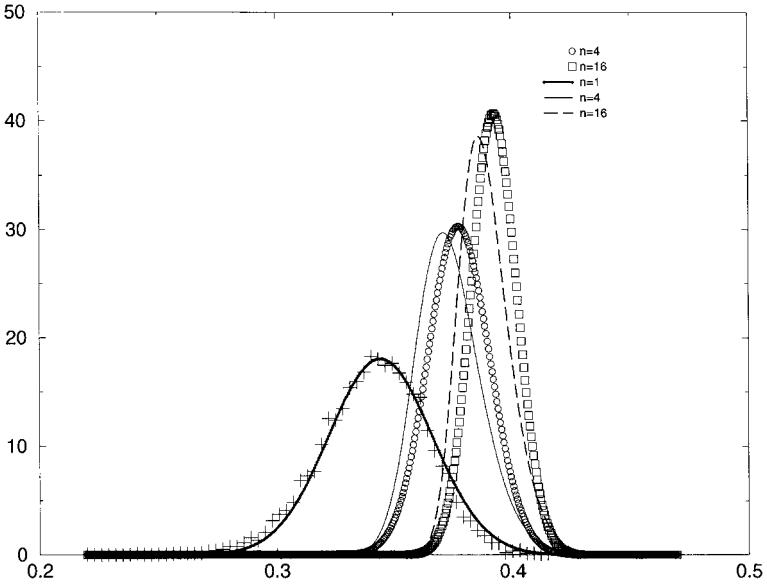

Figure 7. Distribution of terminal threshold for TIP in 3D for $L = 16$. (+) Numerical data $n = 1$ system and a gaussian fit to the data. Lines give the theoretical prediction via Equation (7) for larger n and the data points numerical data.

4.2. NUMERICAL RESULTS

4.2.1. *Confirmation of Scaling for Random TIP*

We first confirm that the scaling predictions derived previously for RP can be extended to IP with trapping. In Figure 7 we show that the distribution of S_r for TIP on an elongated lattice is approximately given by Equation (7). As S_r of TIP and p_c of RP are related (Wilkinson and Willimsen, 1983), one might expect the scaling

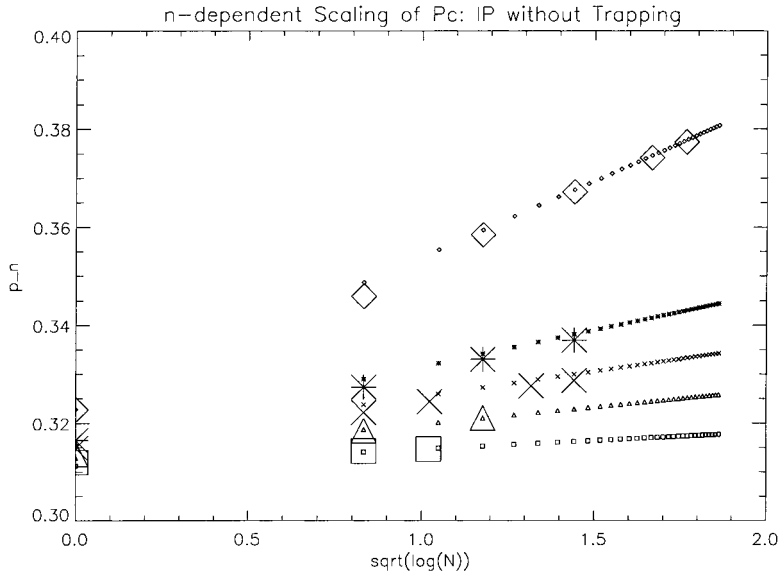

Figure 8. n-dependent scaling of the residual saturation. ($\Diamond$), $L = 16$; ($*$), $L = 32$; (x), $L = 45$; ($\triangle$), $L = 64$; ($\square$), $L = 128$. The larger symbols give the results of the numerical simulation, and the smaller symbols are the theoretical prediction for the scaling of the residuals with n based on Equation (8).

given by Equation (8) derived for RP to be valid for TIP. We show in Figure 8 that this is indeed the case. The fit to Equation (8) is excellent for all L. We note that when the lattice size $L > 100$, the effect of extending the lattice on S_r is minimal. As discussed in Section 3.3, the variance σ of $P(p)$, decreases dramatically with L; $\sigma \propto L^{-a}, a > 1$. The scale of a true core sample is usually greater than 100^2 pores in the normal plane. This result shows that there is little problem in using the results for elongated lattices if the pore space is uncorrelated.

4.2.2. *Confirmation of Scaling for Correlated TIP*

For correlated lattices, the variance in the distribution of S_r is much larger than in the correlated case, and the tails of the distribution are strongly skewed to higher S_r; particularly for the case $\ell_c = L$. Since it is this part of the distribution that is critical in determining the expectation value of S_r^{ext}, we attempt to fit a curve to the higher end of the distribution. Fits to the realised distribution of S_r are given in Figure 9 for lattices of $L = 64$. In Figure 9(a) where correlations extend out to $l_c = 8$, we find the best fit to the tails of the distributions at the high end of $P(S_r)$ gives $a \simeq 1.5$. When the correlations extend to the scale of the core $\ell_c = L$, we find $a \simeq 0.9$.

According to Equation (10) the scaling of the termination threshold is now much more strongly dependent on n. Coupled with a larger variance, we expect a much stronger dependence of S_r^{ext} on n. This is observed in the simulation results. In

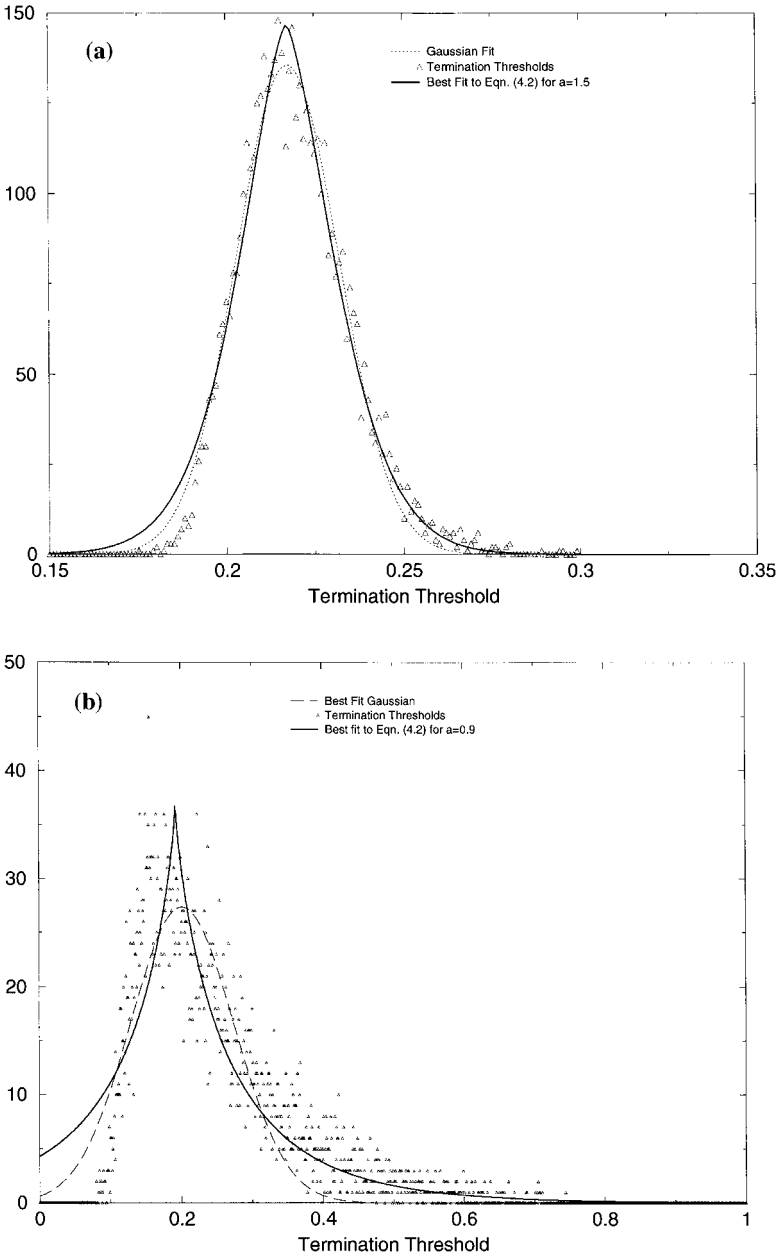

Figure 9. Distribution of termination thresholds for lattices with correlated heterogeneity: (a) $L = 64$, $\ell_c = 8$, (b) $L = 64$, $\ell_c = 64$.

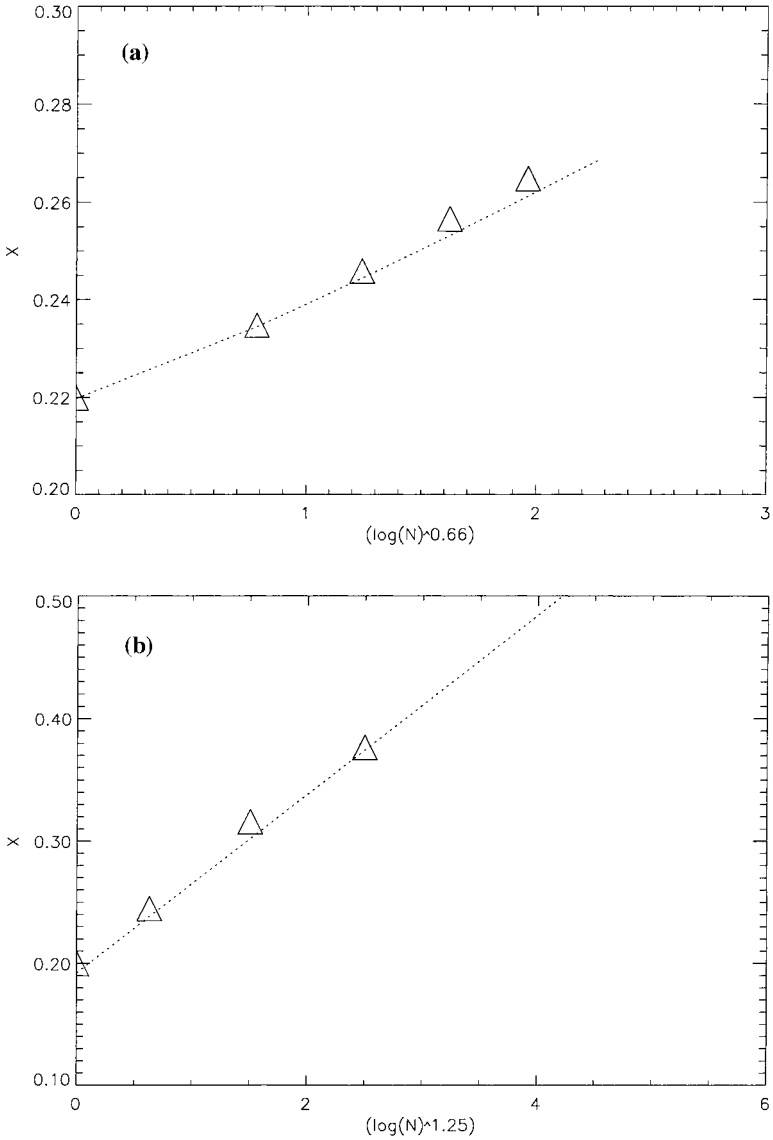

Figure 10. n-dependence of the termination threshold for (a) $L = 64$, $\ell_c = 8$, (b) $L = 64$, $\ell_c = 64$. Data points are results from simulation, and the lines are predictions of Equation (10).

Figure 10 we show the n dependence of S_r^{ext} at a core scale ($L = 64$) for the two systems shown in Figure 9. For short-range correlations ($\ell_c = 8$) we observe a significant ($\simeq 20\%$) change in the residual saturation for an aspect ratio of 10. In the case $\ell_c = L$, for an aspect ratio of $n = 8$ we see an increase in the observed residual of nearly 100%. Figure 10 also shows the predicted scaling behaviour of S_r with n given by Equation (10). The numerical data confirm this general scaling relation for correlated lattices. Our results suggest that studies on lattices with a

high aspect ratio will lead to a significant overestimation of the residual saturation when compared to studies on cubic lattices.

5. Summary

The main results of our study can be summarized as follows:

1. Even small scale correlations have a profound effect on the residual saturation measured at large scales. Previous work (Knackstedt *et al.*, 1998) has shown that correlated heterogeneity exists down to the pore scale even in a rock which is generally considered to be homogeneous. Results of IP simulations on random lattices will provide poor estimation of residuals for such rocks.
2. Introduction of correlated heterogeneity has a strong effect on the resultant distribution of clusters of trapped phase. For small-scale correlations we observe a higher proportion of the residual phase residing in larger trapped clusters. For large-scale correlations one or two trapped clusters account for much of the residual saturation. This may have important implications to tertiary displacements in which a third phase is injected to further reduce the residual saturation. The presence of larger residual clusters may make it easier to reconnect and recover the trapped phase.
3. From an analysis of the scaling behaviour of the variance of the residual saturation, we find that the measurement of residual saturations must be made on samples that are at least 10 times larger than the extent of the correlated heterogeneity. Experiments on Berea sandstone and simulation of porosimetry on correlated lattices (Knackstedt *et al.*, 1998) have provided evidence that correlations persist out to several millimeters even for rocks generally considered to be homogeneous (such as Berea sandstone). Based on this criterion core measurements performed at the centimeter scale on Berea sandstone would not exhibit large fluctuations in the residual saturation and a small number of laboratory displacement tests will produce representative residual saturation values. In preliminary experiments on more heterogeneous rock (Senden *et al.*, to be submitted) we have measured correlations at the scale of several centimeter – the scale of a laboratory core sample. Measurements on such core samples would be expected to produce a wide range of residual saturation values. This expectation is consistent with actual laboratory measurements in which the range of residual oil saturations was between 22% and 42% for a set of six core samples (Paterson *et al.*, 1997).
4. We have derived the scaling of the residual saturation on an elongated lattice exhibiting different scales of correlated heterogeneity. For systems exhibiting uncorrelated heterogeneity, the effect of measuring saturations along an elongated core is minimal. For systems exhibiting correlated heterogeneity there is a significant overestimation of saturation when compared with the corresponding saturation determined on a cubic lattice. This result suggests that considerable caution should be exercised in the application of residuals measured on high

aspect ratio cores. The objective of reducing end effects in short core tests may be countered by the effects of increased residual saturation resulting from increased aspect ratio.

Acknowledgements

M.A. Knackstedt thanks the Australian Research Council for support and the Australian National University Supercomputing Facility for computer time. Work at University of Southern California was supported in part by the Petroleum Research Fund, administered by the American Chemical Society.

References

Dias, M. and Wilkinson, D.: 1986, Percolation with trapping, *J. Phys. A* **19**, 3131–3146.

Du, C., Satik, C. and Yortsos, Y.: 1996, Percolation in a fractional brownian motion lattice, *AIChE J.* **42**, 2392–2394.

Haas, U.: 1995, The distribution of percolating concentrations in finite systems, *Physica A* **215**, 247–250.

Hewett, T.: 1986, Fractal distributions of reservoir heterogeneity and their influence on fluid transport, Technical report, Society of Petroleum Engineers Paper 15836.

Hoshen, J. and Kopelman, R.: 1976, Percolation and cluster sizes, *Physical Rev. B* **14**, 3438.

Knackstedt, M. A., Sheppard, A. P. and Pinczewski, W. V.: 1998, Simulation of mercury porosimetry on correlated grids: Evidence for extended correlated heterogeneity at the pore scale in rocks, *Phys. Rev. E Rapid Communications* **58**, R6923–R6926.

Knackstedt, M. A., Sahimi, M. and Sheppard, A. P.: 2000, Invasion Peredation with long-range correlations: First order phase transition and non-universal scaling properties, *Phys. Rev. E.* **61**, 4920–4934.

Larson, R., Scriven, L. E. and Davis, H. T.: 1977, Percolation theory of residual phases in porous media, *Nature* **268**, 409–413.

Makse, H. A., Ivanov, P. C., Havlin, S., King, P. R., Prakash, S. and Stanley, H.: 1996, Pattern formation in sedimentary rocks: Connectivity, permeability and spatial correlations, *Physica A* **233**, 587–605.

Marrink, S. J., Paterson, L. and Knackstedt, M.: 1999, Definition of percolation thresholds on self-affine surfaces, *Physica A* (P. accepted).

Marrink, S. J. and Knackstedt, M. A.: 1999, Percolation thresholds on elongated lattices, *J. Phys. A Lett.* **32**, L461–L466.

Marrink, S. J. and Knackstedt, M. A.: 2000, Finite size scaling for percolation on elongated lattices in two and three dimensions, *Phys. Rev. E.*, to appear September issue.

Meakin, P.: 1991, Invasion percolation on substrates with correlated disorder, *Physica A* **173**, 305–324.

Mehrabi, A., Rassamdana, H. and Sahimi, M.: 1997, Characterization of long-range correlations in complex distributions and profiles, *Phys. Rev. E* **56**, 712–722.

Painter, S.: 1995, Random fractal models of heterogeneity: the lévy-stable approach, *Mathematical Geology* **27**, 813.

Painter, S.: 1996, Stochastic interpolation of aquifer properties using fractional lévy motion, *Water Resour. Res.* **32**, 1323.

Painter, S. and Paterson, L.: 1994, Fractional lévy motion as a model for spatial variability in sedimentary rock, *Geophys. Res. Lett.* **21**, 2857.

Paterson, L., Painter, S., Zhang, X. and Pinczewski, W. V.: 1997, Simulating residual saturation and relative permeability in heterogeneous formations, *SPE* **36523**.

Sahimi, M.: 1993, Flow, dispersion, and displacement processes in porous media and fractured rocks: From continuum models to fractals, percolation, cellular automata and simulated annealing, *Rev. Mod. Physics* **65**, 1393–1534.

Sahimi, M.: 1994, *Applications of Percolation Theory*, London, Taylor and Francis, first edition.

Sahimi, M.: 1998, Non-linear and Non-local transport processes in heterogeneous media: From long-range correlated percolation to fracture and materials breakdown, *Physics Reports* **306**, 213.

Sahimi, M., Rassamdana, H. and Mehrabi, A.: 1995, Fractals in porous media: From pore to field scale, *Proc. Materials Res. Soc.* **367**, 203–214.

Sahimi, M. and Mukhopadhyay, S.: 1996, Scaling properties of a percolation model with long-range correlations, *Phys. Rev. E* **54**, 3870.

Senden, T. J., Knackstedt, M. A., Sheppard, A. P. and Pinczewski, W. V.: Sedimentary rocks exhibits long-range correlations at the pore scale, *Geophys. Res. Lett* (to be submitted).

Schmittbuhl, J., Vilotte, J.-P. and Roux, S.: 1993, Percolation through self-affine surfaces, *J. Phys. A* **26**, 6115–6133.

Sheppard, A. P., Knackstedt, M. A., Pinczewski, W. V. and Sahimi, M.: 1999, Invasion percolation: new universality classes, *J. Phys. A. Lett.* (submitted).

Sheppard, A. P and Sok, R. M.: Fast algorithm for trapping and searching in invasion percolation, submitted to Transp. in Porous Media.

Stauffer, D. and Aharony, A.: 1994, *Introduction to Percolation Theory*, London, Taylor and Francis, second edition.

Wagner, G., Meakin, P., Feder, J. and Jossang, T.: 1997, Invasion percolation on self-affine topographies, *Phys. Rev. E.* **55**, 1698–1702.

Wilkinson, D. and Willimsen, J.: 1983, Invasion percolation: A new form of percolation theory, *J. Phys. A: Math. Gen.* **16**, 3365–3376.

Ziff, R. M.: 1994, Reply to comment on Spanning Probability in 2D percolation, *Phys. Rev. Lett.* **72**, 1942.